Separation Science and Technology
Publication details, including instructions for authors and subscription information:
http://www.informaworld.com/smpp/title~content=t713708471

Kinetics of Boron Sorption and Desorption in Boron Thermal Regeneration System

Jidong Lou[a]; Gary L. Foutch[a]; Jung Won Na[b]
[a] SCHOOL OF CHEMICAL ENGINEERING, OKLAHOMA STATE UNIVERSITY, STILLWATER, OKLAHOMA, USA [b] KOREA ATOMIC ENERGY RESEARCH INSTITUTE, YUSUNG, SOUTH KOREA

To cite this Article Lou, Jidong , Foutch, Gary L. and Na, Jung Won(2000) 'Kinetics of Boron Sorption and Desorption in Boron Thermal Regeneration System', Separation Science and Technology, 35: 14, 2259 — 2277
To link to this Article: DOI: 10.1081/SS-100102101
URL: http://dx.doi.org/10.1081/SS-100102101

SEPARATION SCIENCE AND TECHNOLOGY, **35**(14), pp. 2259–2277, 2000

Kinetics of Boron Sorption and Desorption in Boron Thermal Regeneration System

JIDONG LOU and GARY L. FOUTCH*
SCHOOL OF CHEMICAL ENGINEERING
OKLAHOMA STATE UNIVERSITY
STILLWATER, OKLAHOMA 74078, USA

JUNG WON NA
WATER CHEMISTRY TECHNOLOGY PROJECT
KOREA ATOMIC ENERGY RESEARCH INSTITUTE
YUSUNG, SOUTH KOREA 305-600

ABSTRACT

Boron is used in the primary coolant of pressurized water reactors in nuclear power generation for shim control. If boron concentration is decreased, fewer neutrons are adsorbed and more fission occurs. When boron concentration increases, less fission occurs. The boron concentration can be controlled by the use of ion-exchange resins operating in the Boron Thermal Regeneration System (BTRS). A better understanding of BTRS kinetics can enhance its potential use for chemical shim control. The concentration and temperature effects on boron sorption and desorption with Amberlite IRN-78LC resins are investigated both experimentally and theoretically for BTRS operating conditions from 0.1–0.2 mol/dm^3 boron and 10–60°C. A model, based on a postulated boron-sorption mechanism, assuming linear driving force through the film with fast, reversible, local reaction equilibrium, is presented. Comparison with experimental data validates that the model predictions are reasonable. The results are also applicable to other boron ion-exchange systems, such as initial breakthrough predictions from water polishers used in manufacturing microchips.

INTRODUCTION

Boron, as boric acid, can be used for chemical shim control in pressurized water reactors (PWR) used for nuclear power generation. Boron compensates for xenon transients and absorbs neutrons to produce tritium and lithium (1).

---

* To whom correspondence should be addressed.

The process of absorbing neutrons controls the power generation, or shim, rate. With higher boron concentrations, less fission occurs; with lower boron concentration, more fission occurs. Boron serves as a supplemental control to the primary control-rod mechanism. The Boron Thermal Regeneration System (BTRS) can control boron concentration because borate is absorbed on ion-exchange resins at low temperature and released at higher temperature. The amount of reactor coolant reprocessed is minimized, whereas reactor coolant chemistry control is improved. BTRS is not currently operational because of the lack of boron sorption and desorption characterization (2). This paper addresses this current technical deficiency by presenting a model that can allow BTRS performance simulation.

Suitable resins are the key to BTRS technology. In large-scale cooling-water treatment, strong base resins with 8–12% divinylbenzene (DVB) crosslinking (3) are most widely used. Resin requirements include higher equilibrium capacity with temperature dependency, good thermal stability, and resistance to radiation damage. Peterka (4) concluded that only strongly basic resins are suitable for BTRS, and Amberlite IRN 78 is economical in commercial use. His work was confirmed by Na (5).

Boron sorption and desorption experiments on strong anion resins are reported by Tomizawa (6–8), Kononova et al. (9), and Na (2, 5). Data from kinetic experiments using Diaion SAN-1 resin (OH^- form) for boron sorption at low temperature and desorption at higher temperature were analyzed using the shrinking-core model (6–8). Activation energy of about 3 and 7 $kcal/mol^{-1}$ for early- and late-stage reaction, respectively, were found during sorption on borate-form resin with concentrations from 0.0231 to 0.463 M. These data suggest that the rate-determining step might switch from early film diffusion to particle diffusion as sorption proceeds. Kononova and his coworkers, with ANB-11G resin at 0.0162 M boron, reached a similar conclusion that diffusion is the limiting step in boron sorption. They also found that the sorption rate is influenced strongly by bead size, and could increase with increasing temperature. Na investigated boric acid sorption on Amberlite IRN-78LC resin at typical BTRS operating conditions. He suggested that the sorption isotherm should consider both the exchange of borate ions and adsorption of nondissociated boric acid. Na found that the diffusion-coefficient temperature dependency of boric acid within the resin follows an Arrhenius form. No quantitative theories have previously been advanced for the kinetics of boric acid sorption or desorption in BTRS.

The theoretical study of BTRS includes sorption equilibrium, kinetic behavior, and column dynamics. The nature of the equilibrium relationship is typically nonlinear and favorable over the operation concentration and temperature ranges (10). The kinetic behavior of boron sorption is complicated; the apparent capacity is both temperature and concentration dependent, and various boron forms exist within the solution phase that are accompanied by multiple reversible reactions that are a function of pH and concentration. In addition, different diffusion patterns exist for both ionic and molecular species through the film and particle. The Nernst-Planck model, used to describe the migration of strong electrolytes, is questionable for this system (11).

This work investigates boron sorption and desorption kinetics on strong base anion resins in BTRS to provide a practical model to predict operation. Conditions addressed are a total boron concentration range near 0.1 to 0.2 mol/dm^{-1}, a temperature range from 10–60°C, and Amberlite IRN 78LC $-$ OH^{-1}-form anion resin. Contributions of both film and intraparticle diffusion resistance will be considered in this model.

THEORY

The sorption of boron on strong base resin seems to be governed by a different mechanism from ordinary ion exchange. A special feature is that polyborate formation occurs at an active site during sorption that results in an increase in equilibrium capacity. If A denotes the counterion initially in the resin (here OH^-), B indicates the boric acid molecule, AB is the tetrahedral $B(OH)_4^-$, and P represents polyborates, the following ion exchanges occur simultaneously in the system.

Process I: Consumption of counterion released by the ion exchanger

$$\overline{RA} + B \longleftrightarrow \overline{RAB} \tag{1}$$

$$\overline{RA} + P + B \longleftrightarrow \overline{RP} + AB \tag{2}$$

Process II: Ion exchange followed by replacement of the tetrahedral ion by polyborates according to selectivity

$$\overline{RA} + AB \longleftrightarrow \overline{RAB} + A \tag{3}$$

$$\overline{RAB} + P \longleftrightarrow \overline{RP} + AB \tag{4}$$

Process III: Complex formation at the exchange site

$$\overline{RAB} + (n-1)B \longleftrightarrow \overline{RAB_n} \tag{5}$$

These reactions may take place at both the interface and at sites within the resin. Hydroxide ions are consumed as soon as they reach the interface by coion H^+, which does not migrate from the bulk to the resin phase because of Donnan exclusion and maintenance of the liquid-phase charge balance.

As boric acid molecules enter the resin phase they react with OH^- to form the tetrahedral $B(OH)_4^-$ because of high, localized pH. Equations (1) to (3) dominate as long as the resin contains enough OH^- for these reactions.

Molecular boric acid migration across the liquid film is rate limiting. As reaction proceeds and sites are converted to the borate form, formation of polyborates at the exchange sites, represented in Eq. (4) and (5), becomes the major reaction. A sharp boundary may result because of slow mobility of boric acid and polyborates inside the resin. Film diffusion control is no longer valid and the rate-controlling step becomes particle diffusion. A reference point to divide the two stages may be chosen, typically when some fraction of the resin capacity exhausts, depending on various operation conditions (8).

Assumptions

The following assumptions, based on system process conditions, are used in the model to minimize mathematical complexity. Boric acid dissociation equilibrium is assumed to obey the equilibrium relationship presented by Mesmer et al. (12–13),

$$\alpha B(OH)_3 + \beta OH^- \xleftrightarrow{K_{\beta\alpha}} B_\alpha\,(OH)^{\beta-}_{\beta+3\alpha} \tag{6}$$

Traces of other borates in solution are neglected. The local equilibrium at the resin–film interface is described by the selectivity relationship. The linear driving force for film and particle-diffusion control, as demonstrated by Glueckauf (14), will be adequate in this study.

In addition, the following common ion-exchange assumptions are used:

- quasi-stationary or pseudo-steady-state film diffusion
- unity activity coefficients
- constant individual diffusion coefficients of the ions and the neutral molecule
- complete Donnan exclusion, no net coion flux within the film
- electrical neutrality
- homogeneous ion-exchanger particles
- negligible swelling changes of the ion exchanger
- neglecting the effect of axial dispersion
- isothermal, isobaric operation

Some assumptions may not be accurate for BTRS, particularly isothermal behavior and absence of swelling changes due to considerable heat produced from the reactions. Concentration may not be uniform because gradients exist near each bead, and flow is nonideal. Moreover, mass transfer varies with time and space. However, the variations of concentration with location in the film are much more important than with time, implying pseudo-steady-state exchange. Models derived with these assumptions represent an approximate rate law.

MODEL DEVELOPMENT

Molecular flux is described by Fick's first law for film-diffusion control

$$J_{HB} = -D_{HB} \bigtriangledown C_{HB} \tag{7}$$

If a linear driving force is applied at the liquid side, Eq. (7) can be expressed as

$$J_{HB} = -k_L \, (C^{\circ}_{HB} - C^{*}_{HB}) \tag{8}$$

where k_L is the mass transfer coefficient of molecular boric acid on the liquid side, which can be determined by an empirical expression, such as the Dwivedi-Upadhyay correlation (15)

$$\frac{k_L}{u} Sc^{2/3} = \frac{1}{\varepsilon}\left(\frac{0.765}{\mathrm{Re}^{0.82}} + \frac{0.365}{\mathrm{Re}^{0.386}}\right) \tag{9}$$

Ionic species flux can be written using the Nernst-Planck equation, as

$$J_i = -D_i\left[\frac{\partial C_i}{\partial r} + z_i \frac{FC_i}{RT} \frac{\partial \Phi}{\partial r}\right] \tag{10}$$

Through the equilibrium relationship in Eq. (6) the relative concentration between borate containing *i* boron molecules to boric acid is

$$C^{i}_{HB} = \frac{1}{k_i K_w^{|z_i|}} C_i C_H^{|z_i|} = \frac{1}{K_i} C_i C_H^{|z_i|} \tag{11}$$

The electrical potential term in Eq. (10) can be replaced by the coions concentration gradient (no coions flux and no net electrical current). In this system, the only coion is hydrogen. Thus, Eq. (11) can be rewritten as

$$J_i = -D_i\left[\frac{\partial C_i}{\partial r} - z_i \frac{C_i}{C_H} \frac{\partial C_H}{\partial r}\right] \tag{12}$$

Differentiation of Eq. (12) leads to the concentration gradient relationship among borate, boric acid, and hydrogen

$$\frac{\partial C_i}{\partial r} = K_i \frac{i \cdot C^{i-1}_{HB}}{C_H^{|z_i|}} \frac{\partial C_{HB}}{\partial r} - \frac{|z_i| C_i}{C_H} \frac{\partial C_H}{\partial r} \tag{13}$$

Substituting Eq. (13) and (11) into Eq. (12) the borate flux in terms of bulk boric acid and hydrogen concentrations is

$$J_i = -D_i K_i \frac{i \cdot C^{i-1}_{HB}}{C_H^{|z_i|}} \frac{\partial C_{HB}}{\partial r} \tag{14}$$

Then the total boron flux in the film is

$$J_{BT} = J_{HB} + \sum J_i = -D_e \frac{\partial C_{HB}}{\partial r} \tag{15}$$

where the apparent diffusivity is

$$D_e = -\left(D_{HB} + \sum D_i K_i \frac{i \cdot C_{HB}^{i-1}}{C_H^{|z_i|}}\right) \tag{16}$$

The particle exchange rate can then be expressed as

$$\frac{d\bar{q}}{dt} = a_s k_L D_e \cdot (C_{BT}^{o} - C_{BT}^{*}) \tag{17}$$

The film-diffusion rate is determined once the total boron interfacial concentration is specified.

For particle-diffusion control, the total boron-exchange rate can be expressed analogous to Eq. (17)

$$\frac{d\bar{q}}{dt} = \bar{k}_e\,(q^* - q) \tag{18}$$

which is subject to the initial condition

$$\bar{q} = \bar{q}_o, \qquad \text{at} \qquad t = t_o \tag{19}$$

Errors from this approach are smaller than expected (16) and can be minimized by an appropriate correlation for the equivalent mass transfer coefficient. Glueckauf (14) first pointed out the equivalence between a linear-rate and diffusion model and derived, for a linear system, the equivalent mass transfer coefficient expression

$$\bar{k}_e = 15\,\frac{\bar{D}_e}{R^2} \tag{20}$$

He validated the expression with various boundary conditions. Comparing theoretical breakthrough curves calculated from the solution of Rosen's diffusion model (17–18), Ruthven (16) showed good agreement with Eq. (20). Therefore, this approximation will be adopted to avoid a complex diffusion model.

Determination of the Bulk Concentrations

There are many ionic borate species, along with molecular boric acid, involved in boron transport from the bulk liquid to the resin (10). Some borate species are unproven in solution at specific conditions. However, borate concentrations are quite low in the BTRS. The problem is simplified because most borate forms do not significantly contribute to the total boron migration toward resins. The clarification of species containing multiple boron molecules and their concentrations is required. The concentration of each borate postulated for a given total boron concentration is determined by combining charge balance, mass conservation, and water dissociation.

The water formation relation

$$K_W = C_{OH} \cdot C_H \tag{21}$$

in combination with borate ionization and equilibrium constants—corresponding to Eq. (6)—results in

$$K_{\alpha\beta} = K_W k_{\alpha\beta} = \frac{[B_{\alpha}^{\beta-}] \cdot [H^+]^{\beta}}{[HB]^{\alpha}} \tag{22}$$

The charge balance and the mass conservation are

$$C_H = C_{B_{11}} + C_{B_{21}} + C_{B_{31}} + 2C_{B_{42}} + C_{OH} \tag{23}$$

$$C_{BT} = C_{HB} + C_{B_{11}} + 2C_{B_{21}} + 3C_{B_{31}} + 4C_{B_{42}} \tag{24}$$

By substituting Eqs. (21) and (22) into Eq. (23) for related species, and solving for C_H, we have

$$C_H = \frac{1}{3}\,(DK_{11}C_{HB} + DK_{21}C_{HB}^2 + DK_{31}C_{HB}^3 + K_W) \tag{25}$$

The concentration of hydroxide can be obtained from Eq. (21) with the result of Eq. (25) by trial and error. With an appropriate initial guess for the boric acid concentration C_B, Eq. (25) can be solved by the Newton-Raphson method. The concentrations of other species are obtained by applying Eq. (22) to each species. Details are given elsewhere (10).

Interfacial Concentrations

The interfacial concentrations at the resin surface are the boundary conditions for the particle rates, and they must relate the equilibrium isotherm defined in this model. If the process is film-diffusion controlled, the concentration distribution within the resin is uniform. When film-diffusion resistance is negligible, the interfacial concentration, C^*, is the bulk liquid concentration. For either limitation, an interfacial concentration occurs at one side of the resistance layer, either from the initial condition or calculation from the column material balance. The boundary condition at the other side of the resistance layer can then be estimated, under the assumption of local equilibrium at the interface, by the following expression (10)

$$Q = a \cdot (C_{BT}^{o})^{\eta} \exp[-(bT + cT^2)] \tag{26}$$

For film-diffusion control, the average boron concentration in the resin $\bar{q}$ replaces the total apparent capacity, Q, and the liquid interface concentration in Eq. (26) becomes

$$C_{BT}^{*} = \left[\frac{\bar{q}}{a} \exp(bT + cT^2)\right]^{1/\eta} \tag{27}$$

Eqs. (21) to (25) are applied to estimate the concentration of other species at the interface.

Similarly, the interface concentration on the resin side in Eq. (18) is expressed, for particle-diffusion control, as

$$q^* = a \cdot (C_{BT}^{o})^{\eta} \exp[-(bT + cT^2)] \tag{28}$$

Column Dynamics

In an ion-exchange column, the equilibrium isotherm determines the nature of the concentration front, and the sharpness of the profile is linked largely to kinetics. The movement of the concentration front, or mass transfer zone, and its response to a perturbation in the feed conditions are described by the overall material balance throughout the column.

In a fixed-bed column, with ideal plug flow and no axial dispersion, the differential boron material balance for a column element of fluid is given as

$$\frac{\partial C_{BT}}{\partial t} + \frac{u}{\varepsilon}\frac{\partial C_{BT}}{\partial z} + \frac{1-\varepsilon}{\varepsilon}\frac{\partial \bar{q}}{\partial t} = 0 \tag{29}$$

subject to the initial and boundary conditions

$$\text{I. C.} \qquad C_{BT} = 0, \qquad q = 0, \qquad \text{at} \qquad t = 0, z = z \tag{30}$$

$$\text{B. C.} \qquad C_{BT} = C_{BT}^{f}, \qquad \text{at} \qquad t = t, z = 0 \tag{31}$$

The term $\frac{\partial \bar{q}}{\partial t}$ is determined by the particle rate expressed generally as

$$\frac{\partial \bar{q}}{\partial t} = F(q, C_{BT}) \tag{32}$$

To obtain the boron front location—or the boron effluent history—Eq. (29) is solved, with initial and boundary conditions [Eq. (30) and (31)], and an appropriate rate equation. Equation (32) is replaced by Eq. (17) for film-diffusion control and Eq. (18) for particle-diffusion control. A porosity ε of 0.35 was used in this work, which is typical in resin-packed columns.

Because all boron forms are interrelated by equilibrium at a given temperature, mass balance equations for each species are not necessary. The concentrations of these species can be readily determined by Eq. (21) through (25) as soon as the total boron concentration is known.

With a dimensionless transform, Eq. (29) and (32) can be rewritten as

$$\frac{\partial X}{\partial \xi} + \frac{\partial Y}{\partial \tau} = 0 \tag{33}$$

$$\frac{\partial Y}{\partial \tau} = f(Y, X) \tag{34}$$

with the initial and boundary conditions

$$\text{I. C.} \qquad X = 0, \qquad Y = 0, \qquad \text{at} \qquad \tau = 0, \xi = \xi \tag{35}$$

$$\text{B. C.} \qquad X = X^{f}, \qquad \text{at} \qquad \tau = \tau, \xi = 0 \tag{36}$$

where the dimensionless parameters are defined as

$$\xi = \frac{k_i\,(1-\varepsilon)}{u}\,\frac{z}{d_p} \tag{37}$$

$$\tau = \frac{k_i C_i^f}{d_p Q}\left(t - \frac{z\varepsilon}{u}\right) \tag{38}$$

$$Y = \frac{\overline{q}}{Q} \qquad \text{and} \qquad X = \frac{C_{BT}}{C_{BT}^f} \tag{39}$$

The explicit form of Eq. (34) in dimensionless form for film-diffusion control is

$$\frac{\partial Y}{\partial \tau} = 6Ri(X^o - X^*) \tag{40}$$

and for particle-diffusion control

$$\frac{\partial Y}{\partial \tau} = 60\gamma(Y^* - Y) \tag{41}$$

where

$$Ri = \left(\frac{D_e}{D_{HB}}\right)^{2/3} \tag{42}$$

$$\gamma = \frac{\overline{D_e}}{k_L d_p}\cdot a\cdot \exp[-(bT + cT^2)]\cdot (C_{BT}^f)^{\eta - 1} \tag{43}$$

Y^* in Equation (41) is not a function of the average fraction, Y, in the resin, but is dependent on the boron feed concentration and can be derived from Eq. (28). As indicated in the assumptions, concentration variations with location in the film are predominant concerns in ion-exchange applications at low concentration. In other words, the pseudo-steady-state exchange could be applied to describe the variations of concentration in the film and on the resin surface. Therefore, integrating Eq. (41) with the initial conditions, the resulting relationship between concentration inside the resin and on the surface can be approximated as

$$Y = Y^*\,[1 - \exp(-60\gamma\tau)] \tag{44}$$

The dimensionless forms are analogous to those used to describe heat transfer in a packed bed, and many of the solutions (19–21) were derived by analogy. Their solutions used infinite-series or error functions, even in some approximate forms. Direct numerical solution of the model equations is applied in this work.

Numerical Solution Techniques

The solution of convective diffusion equations, coupled among different model components, is a major difficulty for simulation of ion-exchange dynamics. Many investigators have applied the method of characteristics to adsorption-packed columns (22), binary and multicomponent ion-exchange columns (23–26), and cation and anion resins in mixed beds (27). This technique is also used in this work.

Equations (33) and (34), which describe, in dimensionless form, the material balance of boron in a column element and the exchange rate around a particle within the element, are coupled first-order ODEs. As soon as the bulk and interface concentrations, and effective diffusivity or equivalent mass transfer coefficients, are obtained, the equations are solved numerically with restrictions in Eqs. (35) and (36).

The assumption that reactions are instantaneous compared to the diffusion rate is applied here. For a small time increment with fast reactions, this approximation is reasonable (28). The boric acid dissociation equilibrium gives algebraic equations solvable by the Newton-Raphson method. The resulting boric acid concentrations are used to determine the effective diffusivity defined in Eq. (16). Euler's and Adams-Bashforth's explicit methods were applied to solve the ODEs. The Runge-Kutta fourth-order method gave the initial starting values for Adams-Bashforth.

EXPERIMENT

Experiments on sorption equilibrium provide data for the determination of Eq. (26) parameters. The detailed experiment work was presented by Na (2). In the experiment, a temperature-adjustable 2600-mL capacity fermentor (Model SY-250, Korea Fermentor Co.) was used as the batch reactor for boric acid adsorption. Reactor temperature was controlled by an ENDOCAL RTE-210 thermostat (NESLAB Co.). Table 1 lists the reactor specifications for adsorption. The resin used was OH^- form Amberlite IRN-78LC with 6% DVB crosslinking (Lot No. 16082). The structure, physical properties, and particle size distribution were examined. The details were provided by Na (2).

The experimental conditions were selected by referencing operation conditions of BTRS. A typical operating temperature of BTRS is 10°C for dilution and 60°C for boration. The concentration of boron in the coolant decreases from about 0.143 M at the beginning of the reactor fuel cycle to about 0.0019 M at the end of the cycle. Therefore, experiments were performed within the

TABLE 1
The Specifications of Reactor Used for Boron-Adsorption Experiment

Contents	Specification
Inside Diameter	132 mm
Height	200 mm
Volume	2600 mL
Number of baffles	3 ea.
Motor (DC)	40 watt
Agitation speed	50–1500 rpm
Heater	30 + 80 watt (2 EA)
Temperature control range	0–60°C
Press of cooling water	0.8–1.2 Kg/cm^2
Materials	Pyrex glass, SUS 316
Power supply	AC 110V, 60 Hz
Model	SY-250
Manufacturer	Korea Fermentor Co

concentration range of 9.25×10^{-5} to 0.143 M boron and temperature range from 10 to 60°C.

To pretreat the resin, it was fully swelled, converted into OH^- form by 2 N NaOH solution, and then rinsed thoroughly with deionized water. After pretreatment, 1000 mL of boric acid solution with given concentration was placed within the batch reactor. The reactor was maintained at a desired temperature ±0.5°C. Then, 8–16 g of pretreated resin were put into the reactor. The system was stirred at 700 rpm for about 2 h. Finally, after adsorption equilibrium was reached, the solution was sampled and analyzed to determine the boron concentration. The data are presented in Table 2 (boron concentration in solution—ppm boron, amount of boron sorbed on the resin—g boron/L), and the sorption isotherms of boric acid on IRN-78LC resin are illustrated in Fig. 1.

Case Comparison and Discussion

The equilibrium concentration on the resin surface is determined by Eq. (28). Values of parameters in the equation were given by Lou, et al. (10). For Amberlite IRN78LC resin, substitution of these values leads to the explicit expression of Eq. (28) as:

$$q^* = 6.30 \times 10^2\, (C_{BT}^o)^{0.291} \exp[-(0.00599T - 4.55 \times 10^{-8}T^2)]$$

Film diffusion dominates the early stage of the exchange process (up to 50% of the intrinsic capacity of the resin), whereas particle diffusion dominates the final stage. A transition point exists where these two mechanisms are equiva-

TABLE 2
Experimental Data of Sorption of Boric Acid on IRN-78LC Resin

10°C		30°C		45°C		60°C	
C ppm	*Q* (g/L)	*C* ppm	*Q* (g/L)	*C* ppm	*Q* (g/L)	*C* ppm	*Q* (g/L)
4.48	10.34	3.95	8.42	7.51	9.1	8.48	8.24
15.86	12.14	5.74	10.06	13.29	10.19	14.85	9.54
45.78	15.37	20.43	12.02	28.56	11.18	71.36	11.64
86.03	17.84	52.57	13.67	81.11	13.44	140.6	13.5
111.5	19.41	111.5	16.72	124.6	16.17	200.4	15.67
324.8	24.31	236.8	19.98	387.2	21.94	344.3	18.12
622.4	28.63	370.3	22.78	706.6	25.10	441.3	19.51
928.6	32.5	680.6	26.52	10.41	27.75	720.1	22.47
1240	36.05	1004	29.80	1392	30.23	1046	25.2
1587	39.57	1331	32.25			1379	27.39
		1440	32.54			1541	28.61

lent. The selection of the switch point is empirical. Tomizawa's work (6–8) and Na's experimental results (2) suggest the switching point is approximately 80–90% of the apparent resin capacity exhausted, depending on the resin type. A value of 80% was used as the transition point in this work for Amberlite IRN78LC resin.

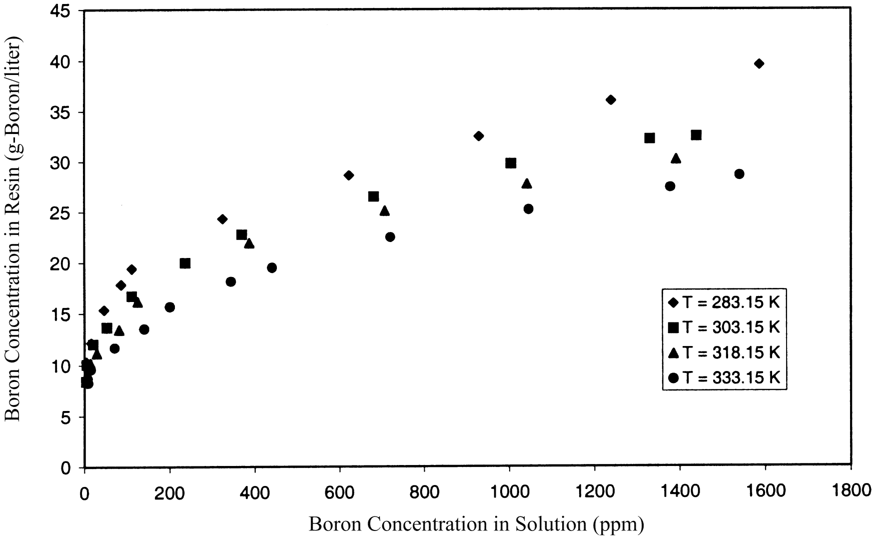

FIG. 1 Sorption isotherms of boric acid on IRN-78LC resin.

The model was tested by comparing data from an industrial plant. In a closed cycle, the initial feed conditions were 463 ppm boron at 17,000 kg/h (for the first 70,000 kg), then flow rate increases to 27,000 kg/h. Boron concentration in the reactor coolant system, after boration, was 246 ppm. The comparison is given in Fig. 2, and the corresponding boron concentration distributions within the column bulk liquid are given in Fig. 3. When the effluent concentration after breakthrough exceeds the feed concentration, boron desorption from the resin occurs to maintain bulk liquid and resin phase equilibrium. Meanwhile, the highest concentration front is located near the most active exchange zone rather than at the column inlet, which reflects boron desorption in the saturated zone as feed concentration decreases. The model did very well predicting column performance.

Some curvature, corresponding to the lower solution concentration range (0–<100 ppm), exists on Fig. 1. This is not a serious challenge to the assumption of a linear driving force applied in this work. We believe that the curvature reflects the contribution of electric potential within the total boron diffusion at very low solution concentrations, which has been shown in past work (27) and accounted for within the effective diffusivity D_e.

The sharp front of these curves indicates that a favorable sorption isotherm and high exchange rate can be expected by using strong base anion resins in

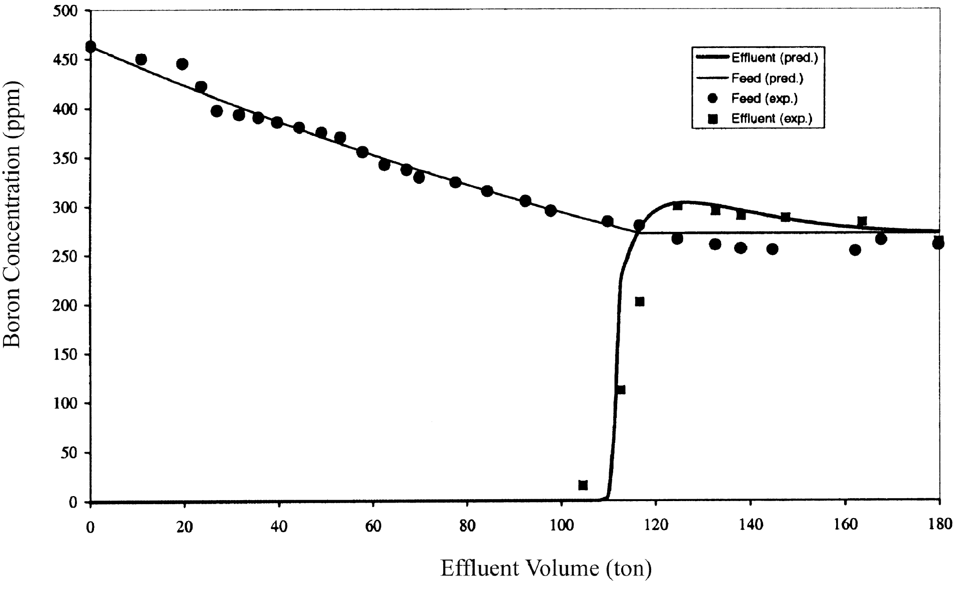

FIG. 2 Comparison of model prediction and operation data for concentration histories in BTRS with conditions: $T = 283$ K, flow rate = 17 M^3/h for 70 M^3, followed by flow rate = 27 M^3/h, Amberlite IRN-78LC resin.

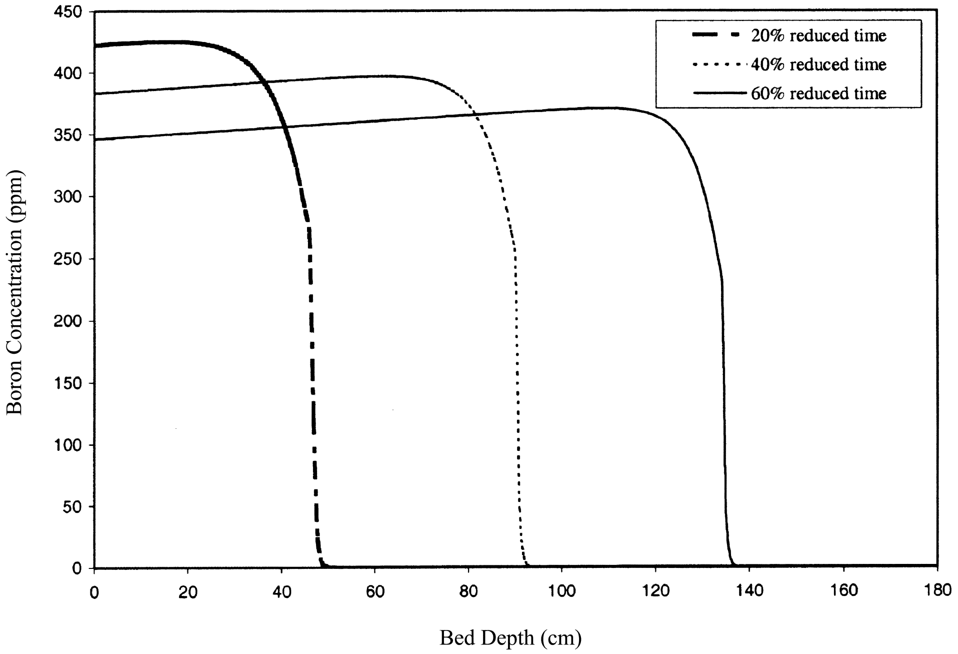

FIG. 3 Boron concentration distributions in the column with time, corresponding to the feed conditions presented in Fig. 2.

BTRS. The sorption behavior can be attributed to

1. dominant boric acid molecular diffusion in the liquid film has less interaction with other diffusing species
2. instantaneous ionization of boric acid molecules at the interface
3. fast polyborate formations inside the resin

However, there is slight deviation in the breakthrough between the experimental data and model prediction in Fig. 2. This deviation could result from either the choice of the transition point or neglecting the effect of axial diffusion or both.

Donnan exclusion leads to no net coion flux within the film, which means that the concentration gradient of hydrogen ions in this case is constant. In other words, the concentration gradients of boric acid molecules and borates are constant due to the equilibrium relations between the boron carriers and hydrogen ions. Fast reversible chemical reactions balance the concentrations among boric acid and various borates in the film. This reduces possible interactions among diffusion species that may produce the resistance to boron carrier transport from the bulk liquid to the interface. The immediate consumption of hydroxide ions released from the resin at the interface partly reduces the interactions of coions.

The instantaneous ionization of boric acid at the interface results in an extremely low concentration of molecular boric acid, which gives the largest possible driving force for the molecular diffusion on the liquid side and accelerates the exchange rate. This can be considered valid when little resin capacity has been consumed. Figure 4 shows the favorable exchange rate as boric acid sorption on IRN-78LC resin in BTRS. The decreased exchange rate after the peak results from boron desorption due to decreasing feed concentration.

The rapid polyborate formation at sites within the resin dramatically increases the apparent (or equilibrium) capacity for boron, and favors formation of a sharp boundary between the interface and the resin interior in the later stages of sorption. This in turn favors a fast exchange rate and the postulation of a linear driving force.

Effects of temperature on boron sorption are indicated in Fig. 5. The exchange rate depends weakly on temperature for the conditions studied because of the weak temperature dependence of mass transfer coefficients and negli-

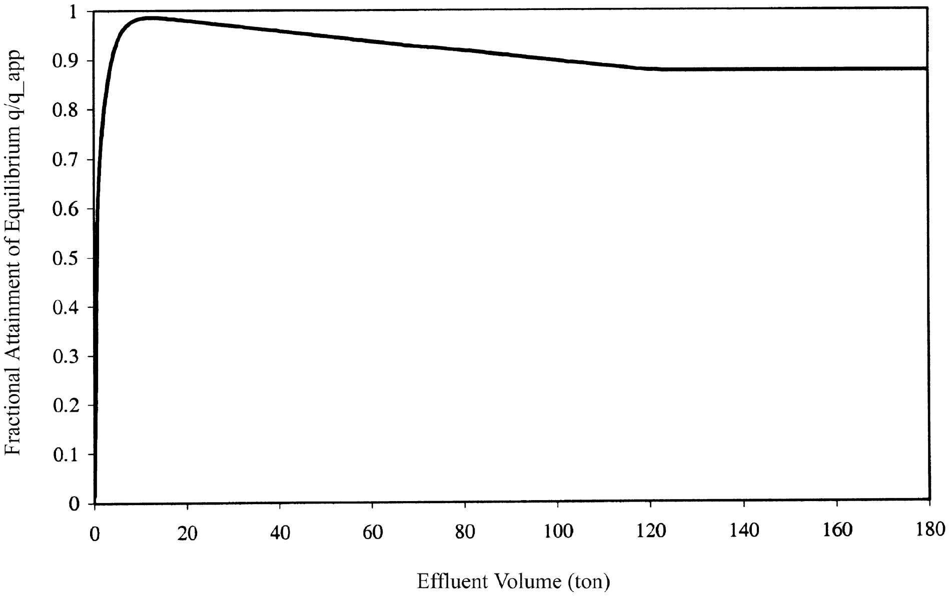

FIG. 4 Uptake of boric acid on Amberlite IRN-78LC resin in BTRS (q = average boron concentration in resin, q_app = apparent capacity corresponding to feed concentration of 463 ppm and temperature of 283 K).

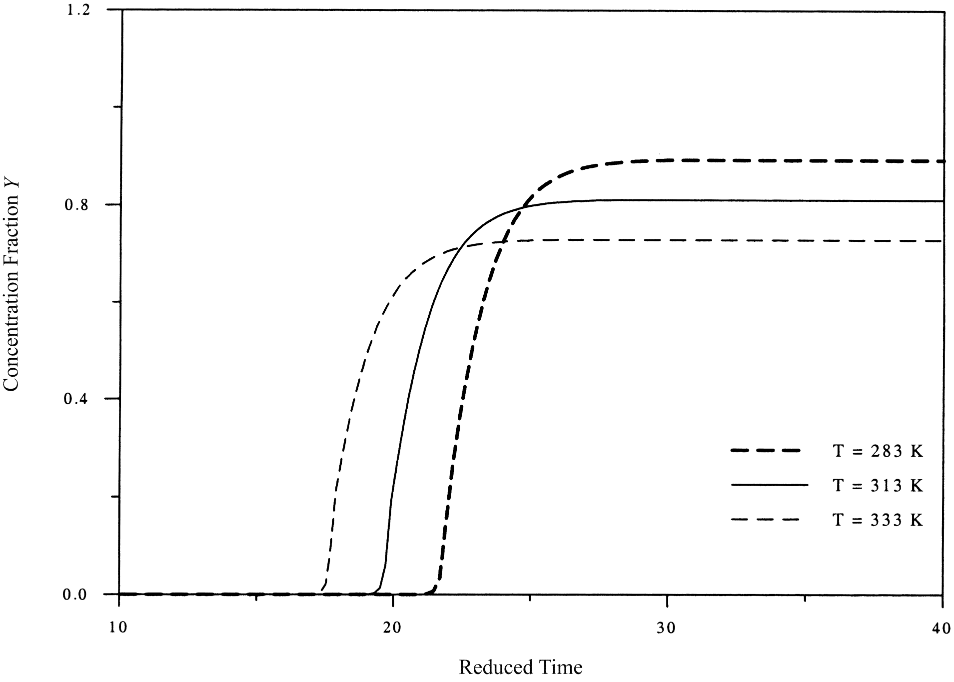

FIG. 5 Effect of temperature on uptake of boric acid on Amberlite IRN-78LC resin and breakthrough.

gible concentration of dissociated ionic species from boric acid at these temperatures.

The apparent resin capacity, however, varies with changing temperature, about 25% higher at 10°C than 60°C. Correspondingly, with similar conditions, the concentration front at higher temperature will be farther down the column than that at lower temperature at a given time, and breakthrough is expected to occur earlier.

CONCLUSIONS

Experiments revealed that the boron sorption on IRN-78LC resin increases with increasing boron concentration and decreases with increasing temperature. The model demonstrates the feasibility of modeling boron sorption in BTRS. The steep shape of the breakthrough curves results from favorable sorption equilibrium of boron on OH^--form anion resin. Lower temperature favors sorption. Dominant molecular migration may allow the simplification of neglecting borates to boron sorption at higher concentrations. If this simplification is used, Fick's law is sufficient for boron sorption kinetics in BTRS. Modeling both molecular and ionic forms is recommended for lower concentrations.

NOMENCLATURE

a	parameter in Eq. (26)	
a_s	specific area of resin	(cm^2/cm^3)
b	parameter in Eq. (26)	
c	parameter in Eq. (26)	
C_i	concentration of *i*th species in solution	(mM/dm^3)
D_e	effective diffusivity of boric acid	(cm^2/sec)
D_i	self diffusivity of *i*th species	(cm^2/sec)
J_i	flux of *i*th species	(mM/cm^2·sec)
k_e	effective mass transfer coefficient of boron	(cm/sec)
k_L	boric acid mass transfer coefficient at liquid side	(cm/sec)
K_i	equilibrium constant of reaction for *i*th species	
q	average boron concentration in resin	(mM/cm^3)
Q	resin equilibrium capacity	(mM/cm^3)
R	universal gas constant	
Re	Reynolds number of particle	
Sc	Schmidt number	
t	time	(sec)
T	temperature	(K)
u	superficial velocity	(cm/sec)
X, Y	concentration fractions in solution and resin	
z_i	charge number of *i*th species	

Greek symbols

α	proportional constant in Eq. (6)
β	proportional constant in Eq. (6)
γ	parameter in Eq. (41)
η	parameter in Eq. (26)
ε	column void fraction
τ	dimensionless time specified in Eq. (38)
ξ	dimensionless space coordinate specified in Eq. (37)

Superscripts

bar	refers to resin phase and average concentration in resin
$*$	interfacial conditions

^{o}	bulk phase conditions
f	refers to feed conditions

Subscripts

$_{o}$	initial conditions
BT	total boron in solution
HB	boric acid
H	hydrogen ions
OH	hydroxide ions
W	water
B_{11}	monoborate
B_{21}	diborates
B_{31}	triborates
B_{42}	tetraborates with charge number −2
α	boron atom number in borates
β	charge number of borates

REFERENCES

1. P. Cohen, *Water Coolant Technology of Power Reactors*, Gordon and Breach Science Publishers, New York, 1969.
2. J. W. Na, "Adsorption Characteristics of Boric Acid on Strong-Base Anion Exchange Resin," *Ph.D. dissertation*, Korea Advanced Institute of Science and Technology, Taejon, Korea, 1993a.
3. K. H. Lin, "Use of Ion Exchange for the Treatment of Liquids in Nuclear Power Plants," *Report ORNL-4792*, Oak Ridge, TN, 1973.
4. F. Peterka, "Selection of Anion Exchange Resins for Boron Thermal Regeneration Systems," *J. Chromatogr., 201*, 359–370 (1980).
5. J. W. Na, "Characteristics of Boron Adsorption on Strong-Base Anion-Exchange Resin," *Ann. Nucl. Energy, 20*(7), 455–462 (1993).
6. T. Tomizawa, "Studies on the Absorption of Boric Acid on Anion Exchange Resins. III. Kinetics of the Absorption of Boric Acid on OH^{-}-Form Anion Exchange Resins," *Denki Kagaku, 49*(8), 503–510 (1981).
7. T. Tomizawa, "Studies on the Absorption of Boric Acid on Anion Exchange Resins. IV. Kinetics of Desorption of Boric Acid from Borate-Form Anion Exchange Resins," *Ibid., 50*(11), 886–891 (1982).
8. T. Tomizawa, "Studies on the Absorption of Boric Acid on Anion Exchange Resins. VII. Adsorption Kinetics of Boric Acid on Borate-Form Anion Exchange Resin," *Ibid., 51*(8), 686–690 (1983).
9. G. N. Kononova, O. A. Plotnikova, A. L. Martyushin, and O. Yu. Odinstov, "Kinetics of the Sorption of Boron by the ANB-11G Resin," *Russ. J. Phys. Chem., 61*(5), 705–707 (1987).
10. J. Lou, G. L. Foutch, and J. W. Na, "The Sorption Capacity of Boron on Anionic Exchange Resin," *Sep. Sci. Technol., 34*(15), 2923–2943 (1999).
11. M. Périé, J. Périé, and M. Chemla, "Nuclear Grade Resins: Kinetics of Isotopic and Ionic Exchange for Borate and Chloride Anions," *J. Electroanal. Chem., 303*, 105–124 (1991).

12. R. E. Mesmer, C. F. Baes Jr., and F. H. Sweeton, "Boric Acid Equilibria and pH in PWR Coolants," *Proceedings of the 32^nd^ International Water Conference*, Pittsburgh, PA, 55–62, 1972.
13. R. E. Mesmer, C. F. Baes Jr., and F. H. Sweeton, "Acidity Measurement at Elevated Temperatures. VI. Boric Acid Equilibria," *Inorg. Chem., 11*(3), 537–543 (1972).
14. E. Glueckauf, "Theory of Chromatography," *Trans. Faraday Soc., 51*, 1540 (1955).
15. P. N. Dwivedi and S. N. Upadhyay, "Particle-Fluid Mass Transfer in Fixed and Fluidized Beds," *Ind. Eng. Chem., Process Des. Dev., 16*(2), 157–165 (1977).
16. D. M. Ruthven, "Principles of Adsorption and Adsorption Processes," Wiley, New York, 1984.
17. J. B. Rosen, "Kinetics of a Fixed Bed System for Solid Diffusion into Spherical Particles," *J. Chem. Phys., 20*, 387 (1952).
18. J. B. Rosen, "General Numerical Solution for Solid Diffusion in Fixed Beds," *Ind. Eng. Chem., 46*(8), 1590 (1954).
19. C. C. Furnas, "Heat Transfer from a Gas Stream to a Bed of Broken Solids," *Trans. Am. Inst. Chem. Eng., 24*, 142 (1930).
20. J. E. Walter, "Multiple Adsorption from Solutions," *J. Chem. Phys., 13*(6), 229–332 (1945).
21. A. Klinkenberg, "Heat Transfer in Cross-Flow Heat Exchangers and Packed Beds," *Ind. Eng. Chem., 46,* 2285 (1954).
22. A. Acrivos, "Solution of the Laminar Boundary Layer Energy Equation at High Prandtl Number," *Phys. Fluids, 3*, 657–658 (1958).
23. J. S. Dranoff and L. Lapidus, "Multicomponent Ion Exchange Column Calculations," *Ind. Eng. Chem., 50*, 1648–1653 (1958).
24. J. S. Dranoff and L. Lapidus, "Ion Exchange in Ternary Systems," *Ind. Eng. Chem., 53*, 71–76 (1961).
25. F. G. Helfferich, *Ion Exchange*, McGraw-Hill, New York, 1962.
26. O. O. Omatete, R. N. Clazie, and T. Vermeulen, "Column Dynamics of Ternary Ion Exchange. II. Solution Mass Transfer Controlling," *Chem. Eng. J., 19*, 241–250 (1980).
27. C. E. Haub and G. L. Foutch, "Mixed-Bed Ion Exchange at Concentrations Approaching the Dissociation of Water. 2. Column Model Applications," *Ind. Eng. Chem. Fund., 25*, 381–385. (1986).
28. Y. L. Wang and F. G. Helfferich, "Generalized Model for Multispecies Ion-Exchange Kinetics Including Fast Reversible Reactions," *Reactive Polymers, 5*, 237–253 (1987).

Received by editor August 5, 1999
Revision received February 2000